Clays and Clay Minerals, Vol. 48, No. 4, 409–423, 2000.

SAPONITE FROM THE EMET COLEMANITE MINES, KÜTAHYA, TURKEY

MÜMTAZ ÇOLAK,[1,2] CAHİT HELVACI,[2] AND MARINO MAGGETTI[1]

[1] Institute of Mineralogy and Petrography, Perolles, 1700 Fribourg, Switzerland
[2] Dokuz Eylül Üniversitesi, Mühendislik Fakültesi, Jeoloji Mühendisliği Bölümü, 35100 Bornova-İzmir, Turkey

Abstract—Clay mineralogy and whole-rock chemistry of the borate-bearing layers of the Hisarcık and Esbey mines were examined. The Hisarcık clays occur as laminated or unlaminated clay layers with sharp contacts. Unlaminated layers contain quartz derived from metamorphic rocks and carbonate fragments in a clay matrix, and are interpreted as reworked tuffs deposited in playa-lake environments. An important feature is that the unlaminated clays contain little MgO (3–15 wt. %) as compared with the laminated clays (15–30 wt. %). As previous studies have shown, the clay fraction of the studied profile contains predominantly Li-bearing saponite, and accounts for 60–90 wt. % of the clay fraction (<2 μm). Illite in the clay fraction varies from 0 to 67 wt. % and the average illite percentage never exceeds 40 wt. %. Chlorite is scarce (2–5 wt. %). Illite-smectite interstratified clays (illite at 70%, smectite at 30%) were only found in low concentrations in the laminated clay layers of the upper limestone unit (above the borate zone), where illite-2*M* of detrital origin is also present. The Esbey clays occur interstratified with colemanite layers and envelope colemanite nodules. Calcite is the major mineral of the clays whereas quartz, plagioclase, feldspar, colemanite, and cahnite are minor components. The MgO contents vary between 4.70–13.95 wt. % in the clays interstratified with colemanite layers, between 7.24–11.89 wt. % in the enveloping clays, and between 10.27–21.25 wt. % in clays located above the colemanite zone. The composition of the clay fraction (<2 μm) in all samples is similar. Smectite represents between 40–90 wt. % of the clay fraction in the upper portion of the stratigraphic profile and decreases towards the lower part of the stratigraphic profile. Smectite always occurs with illite which may vary from 20 to 90 wt. % of the clay fraction, and a small amount of kaolinite and chlorite. Illite-2*M* polytype is abundant. The *d*(060)-reflection position suggests that the smectite minerals from the Hisarcık and Esbey colemanite mines contain both dioctahedral and trioctahedral smectites to form a transitional zone. These smectites are a product of a magnesium-rich alkaline playa-lake environment.

Key Words—Colemanite, Emet, Esbey, Hisarcık, Saponite, Trioctahedral Smectite.

INTRODUCTION

Emet is located 100 km southwest of Kütahya, which was an important ceramic center in Anatolia in the past (Figure 1). Of the two main borate mines in the Emet region, one is the Esbey colemanite mine, 5 km northeast of Emet and the other is the Hisarcık colemanite mine, 11 km south of Emet. The Emet borate mines were first discovered by J. Gawlik (unpubl.) during lignite exploration work for the Mineral Research and Exploration Institute of Turkey (MTA) in 1956. Numerous studies were subsequently conducted on the geology, mineralogy, origin, and reserve of the borate deposits (Özpeker, 1969; Helvacı, 1977, 1983, 1984, 1986; Helvacı *et al.*, 1993; Helvacı and Firman, 1976; Kistler and Helvacı, 1994; Yalçın, 1984; Dündar *et al.*, 1986). The principal borate mineral is colemanite with minor amounts of ulexite, hydroboracite, veachite-A, teruggite, cahnite, tunellite, and meyerhofferite. Native sulfur, realgar, orpiment, and celestite are also present (Helvacı, 1984). Ataman and Baysal (1978) found that the dominant clay minerals are montmorillonite and chlorite. Interstratified clay minerals are rare. Illite is commonly observed in the stratigraphic section, especially in tuff and reworked tuff strata. Helvacı *et al.* (1993) detected boron-bearing K-rich feldspar, clinoptilolite, illite, and smectite as authigenic silicates in the tuffaceous samples. Volcaniclastic high sanidine and quartz are also present. According to Semelin and Yalçın (1984) the tuff, which is composed of glassy rhyolitic ash, was deposited in an inland lake during the volcanic activity. These authors found fresh glass (original rhyolite) + smectite, clinoptilolite + opal CT + smectite, clinoptilolite + quartz + minor smectite, and K-rich feldspar + quartz + smectite assemblages in horizontal zones extending from north to south in the Emet basin. Yalçın and Gündoğdu (1985) conducted the first detailed study on the clay mineralogy of these volcaniclastic sedimentary units. The unit underlying the borate zone of the Emet Formation contains large amounts of zeolites, and it also contains dioctahedral smectite (montmorillonite-beidellite). In contrast, the borate zone contains the trioctahedral smectites, stevensite and Al-rich stevensite. Saponite is observed in the clayey horizons above the colemanite zone in the Hisarcık colemanite mine. According to Yalçın and Gündoğdu (1985), saponite is a neoformation product that was formed as a result of the hydrolysis of volcanic materials in the lacustrine environment. Illite and chlorite were sedimented after transport by aeloian and low-energy fluvial processes.

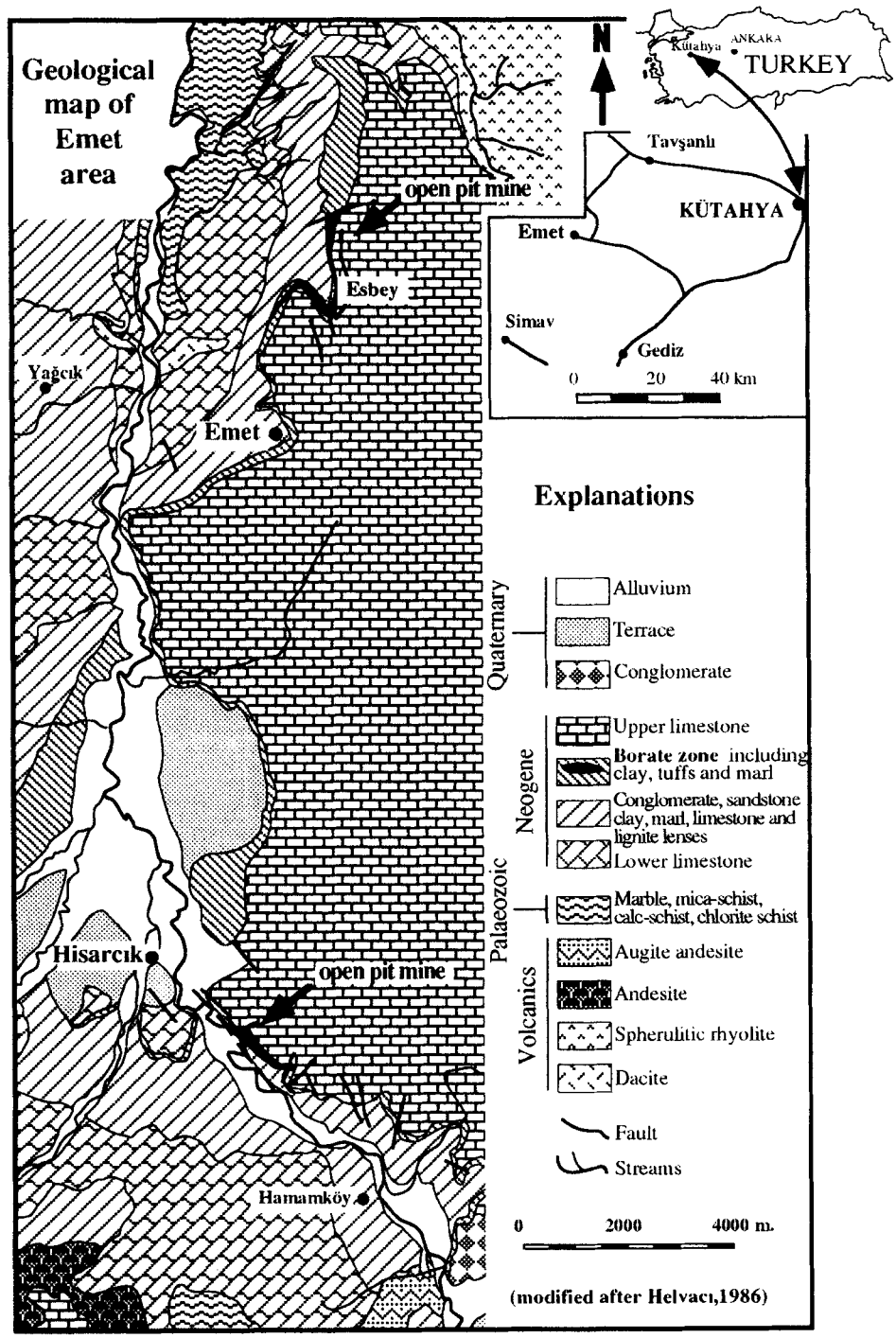

Figure 1. Location and geological map of the Emet borate mine (after Helvacı, 1986).

→

Figure 2. Stratigraphic profile of the Hisarcık colemanite open pit mine. Left side is upper part of the profile, right side is lower part of profile.

https://doi.org/10.1346/CCMN.2000.0480401 Published online by Cambridge University Press

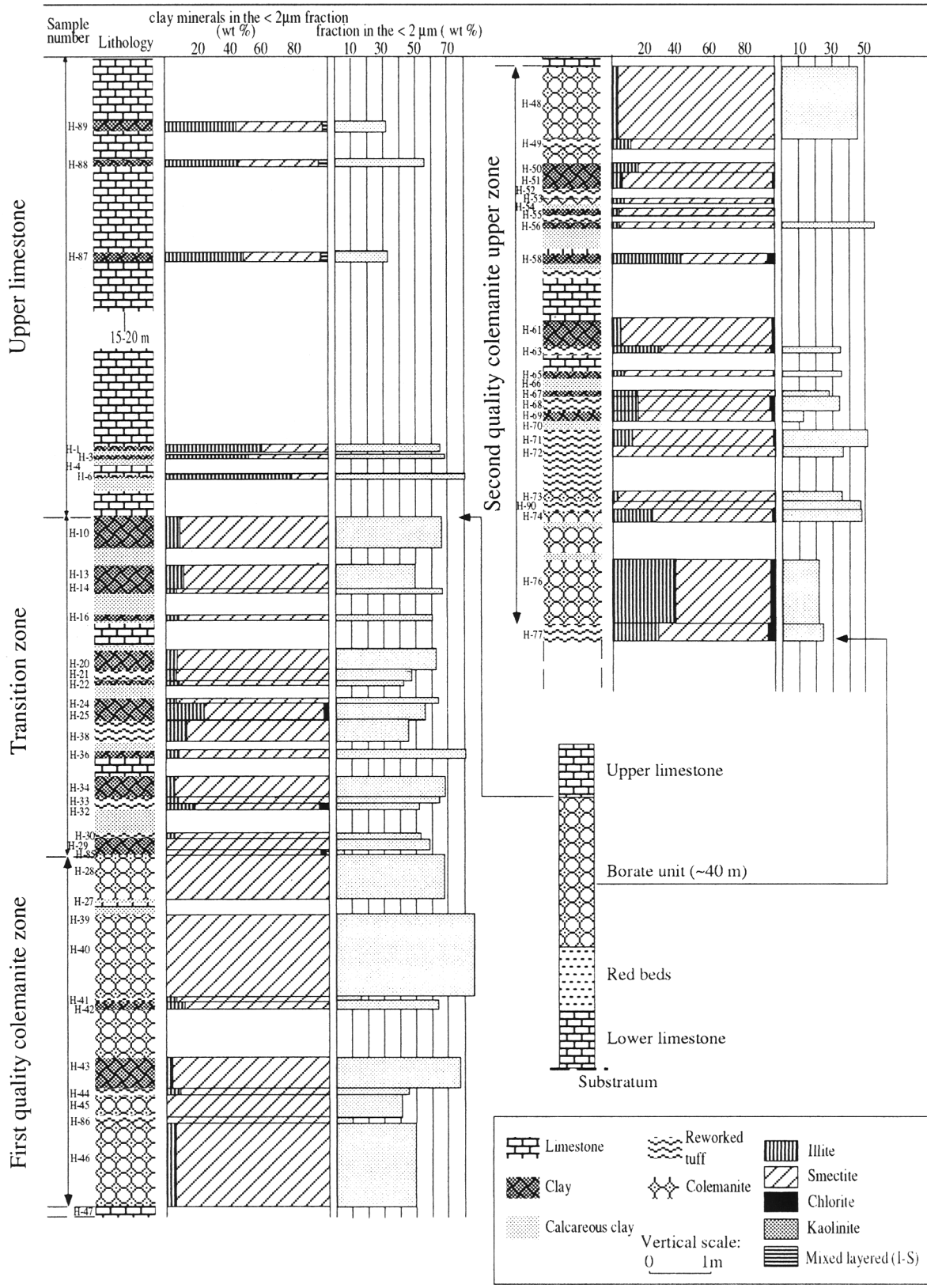

https://doi.org/10.1346/CCMN.2000.0480401 Published online by Cambridge University Press

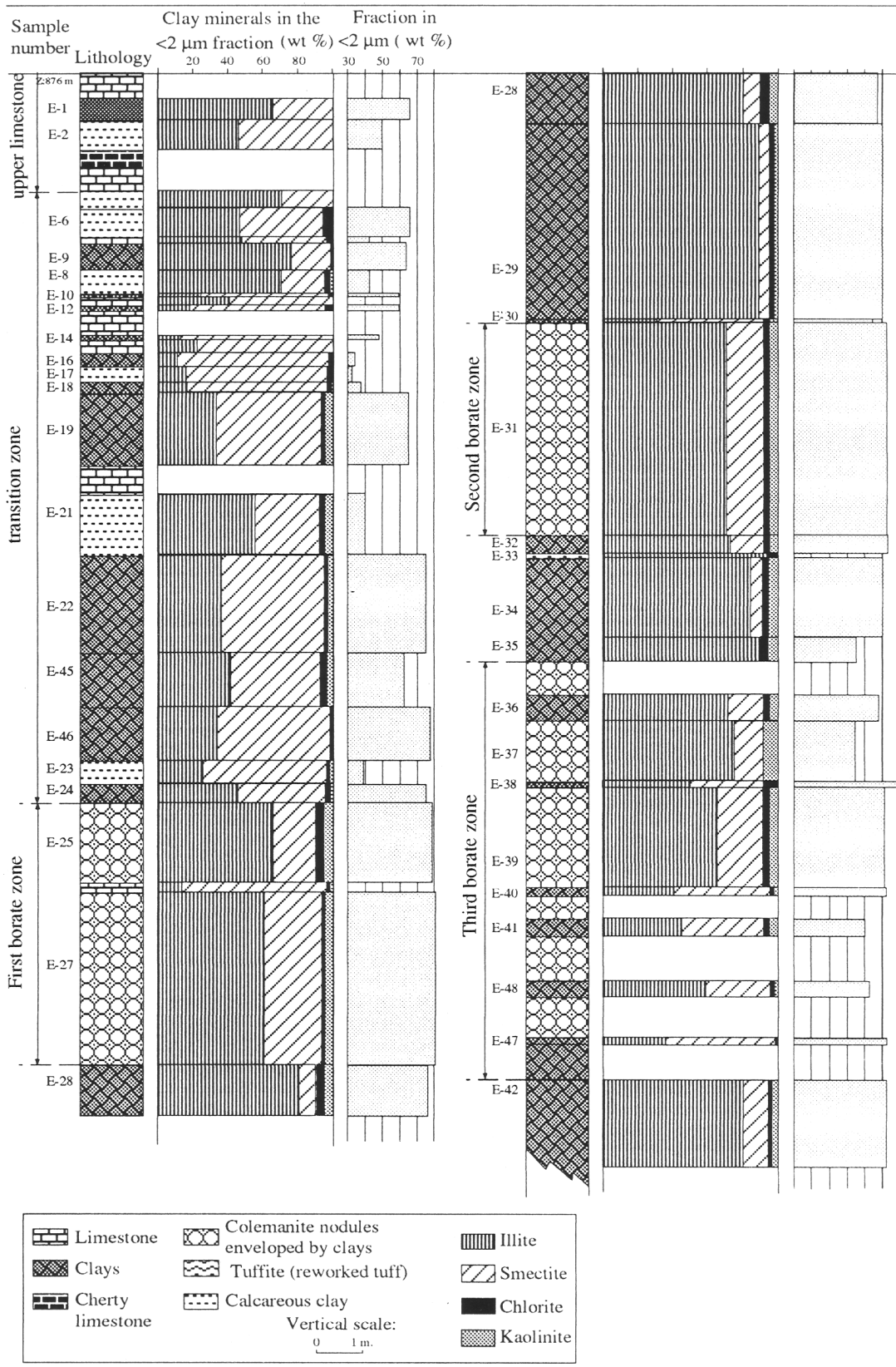

https://doi.org/10.1346/CCMN.2000.0480401 Published online by Cambridge University Press

Table 1. Mineral content of the rock from Hisarcık and Esbey colemanite mines.

Hisarcık colemanite mine		Esbey colemanite mine	
Rock	Mineralogy	Rock	Mineralogy
Limestone	calcite, quartz, K-rich feldspar, plagioclase, orpiment, realgar, and clay minerals (realgar and celestite observed in samples H-60 and H-64)	Limestone	calcite, quartz, cristobalite, (cahnite in sample E-26)
Calcareous clay	calcite, quartz, cristobalite, K-rich feldspar, plagioclase, orpiment, realgar, smectite, illite, and chlorite	Calcareous clay	calcite, quartz, K-rich feldspar, plagioclase, orpiment, realgar, (cahnite in sample E-23), illite, smectite, chlorite, and kaolinite
Clays:		Clays:	
clays over the colemanite zone	calcite, quartz, cristobalite, K-rich feldspar, plagioclase, orpiment, realgar, smectite, illite, chlorite, and kaolinite	clays over the colemanite zone	calcite, quartz, K-rich feldspar, plagioclase, illite, smectite, chlorite, and kaolinite
clay bands interstratified with nodular colemanite layers	calcite, quartz, cristobalite, K-rich feldspar, plagioclase, orpiment, realgar, celestite, smectite, illite, and chlorite	clay bands interstratified with nodular colemanite layers	calcite, quartz, K-rich feldspar, plagioclase, colemanite (samples E-28, E-29, E-34, E-40, E-47), cahnite (E-28), illite, smectite, chlorite, and kaolinite
clays enveloping the colemanite nodules	calcite, quartz, cristobalite, K-rich feldspar, plagioclase, colemanite, realgar, celestite, smectite, illite, and chlorite	clays enveloping the colemanite nodules	quartz, plagioclase, colemanite, illite, smectite, chlorite, and kaolinite
Reworked tuffs	quartz, K-rich feldspar, calcite, colemanite, cristobalite, celestite, orpiment, realgar, smectite, illite, and chlorite	Reworked tuffs	quartz, K-rich feldspar, plagioclase, amphibole, colemanite, biotite, illite, and chlorite

Illite is transformed to illite-smectite (I-S) interstratified clay minerals (Yalçın and Gündoğdu, 1985). After loss of potassium, smectite is formed. Helvacı (1986) suggested that chlorite is formed as a result of alteration of feldspar phenocrysts in tuffs.

The aim of the present paper is to report on the: (1) clay mineralogy and chemistry of the clay-rich and tuffaceous layers; (2) formation of saponite; and (3) relationship of saponite to Mg concentration in the clay-rich and tuffaceous layers at the Hisarcık and Esbey colemanite mines.

MATERIALS AND METHODS

Studies were conducted on a 27-m thick stratigraphic profile for the Hisarcık mine (Figure 2) and on a 44-m thick stratigraphic profile for the Esbey mine (Figure 3). Samples were obtained from the upper limestones to the bottom of the open pit mines. Mineral analyses were performed by X-ray diffraction (XRD) using CuKα radiation (30 kV, 40 mA) on a Siemens Kristalloflex D500 X-ray generator. Random powder samples were prepared for mineral identification and the <2-μm size fraction was separated and oriented clay-aggregate samples were prepared after centrifuging (Gibbs, 1965, 1968). Before preparation of the oriented samples, the carbonate content was determined by dissolution in 2 N HCl for 30 min. Selected samples of the clay fraction were saturated with ethylene glycol for 12 h at 60°C, and heated to 550°C. Each was subjected to XRD analysis. A semi-quantitative analysis of the <2-μm size fraction was obtained by multiplying the intensities of the principal basal reflections of each clay component by suitable factors according to unpublished internal reports of the Institute of Mineralogy and Petrography of the University of Bern. Reproducibility is ±5%. The error is ~20%. XRD patterns of randomly oriented samples were used for polytype analysis. To determine the $1M/2M_1$ ratio, the method as described by Maxwell and Hower (1967) was used where the $d(116)$ intensity of the $2M_1$ phase is compared to the $d(130)$ intensity of the $1M$ phase. The powder sample for the <2-μm size fraction was fixed by alcohol to the glass slide and care was taken to avoid any pressure on the particles. This method does not randomize both phases equally. Fresh, broken surfaces of the undisturbed clay samples

←

Figure 3. Stratigraphic profile of the Esbey colemanite open pit mine. Left side is upper part of the profile, right side is lower part of profile.

https://doi.org/10.1346/CCMN.2000.0480401 Published online by Cambridge University Press

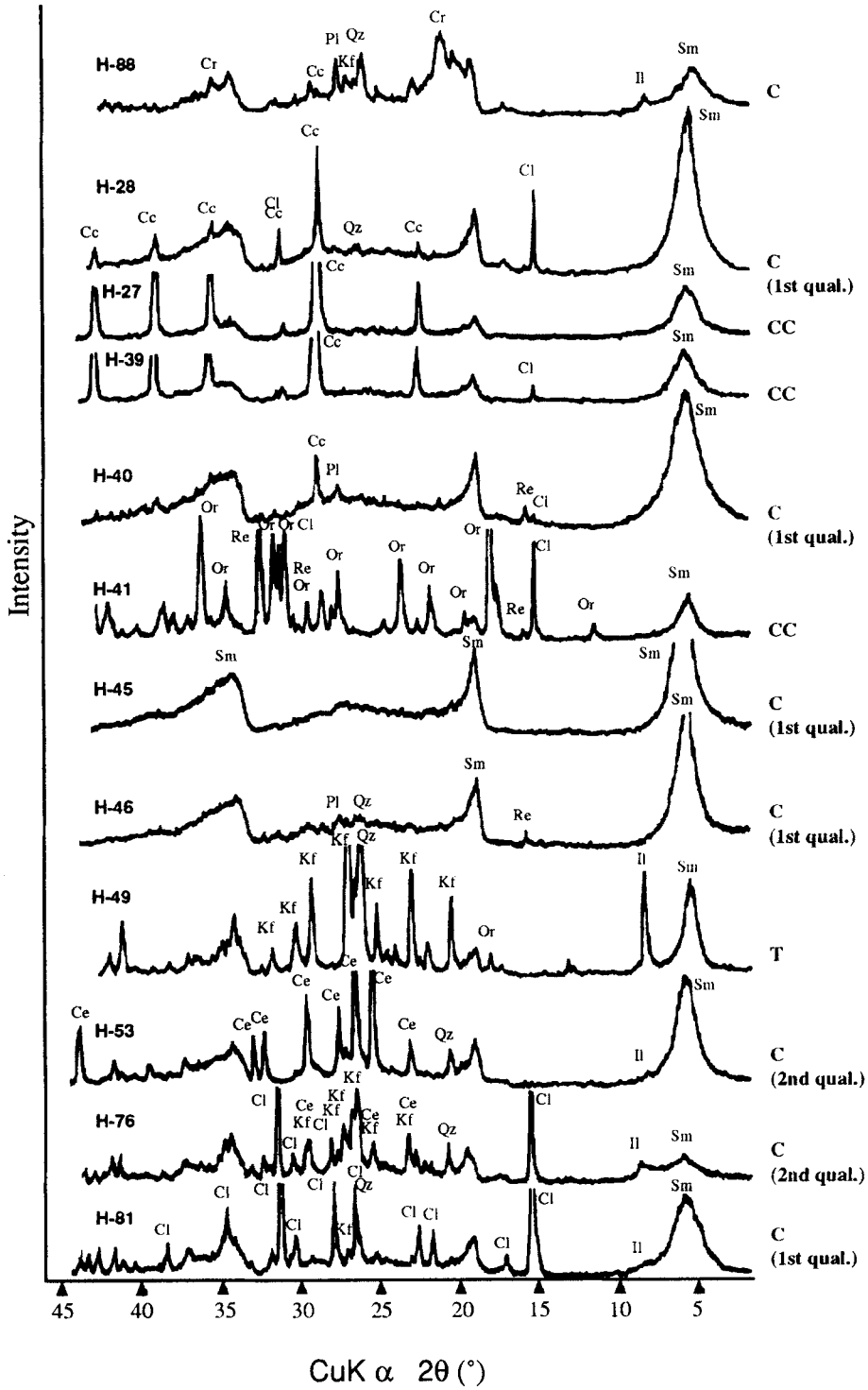

Figure 4. X-ray diffraction patterns of selected bulk samples from the Hisarcık colemanite open pit mine. (Cc: calcite, Qz: quartz, Kf: K-rich feldspar, Cr: cristobalite, Pl: plagioclase, Cl: colemanite, Re: realgar, Or: orpiment, Ce: celestite, Sm: smectite, Il: illite). C: clay, CC: calcareous clay, T: tuffite. Vertical axis is intensity.

https://doi.org/10.1346/CCMN.2000.0480401 Published online by Cambridge University Press

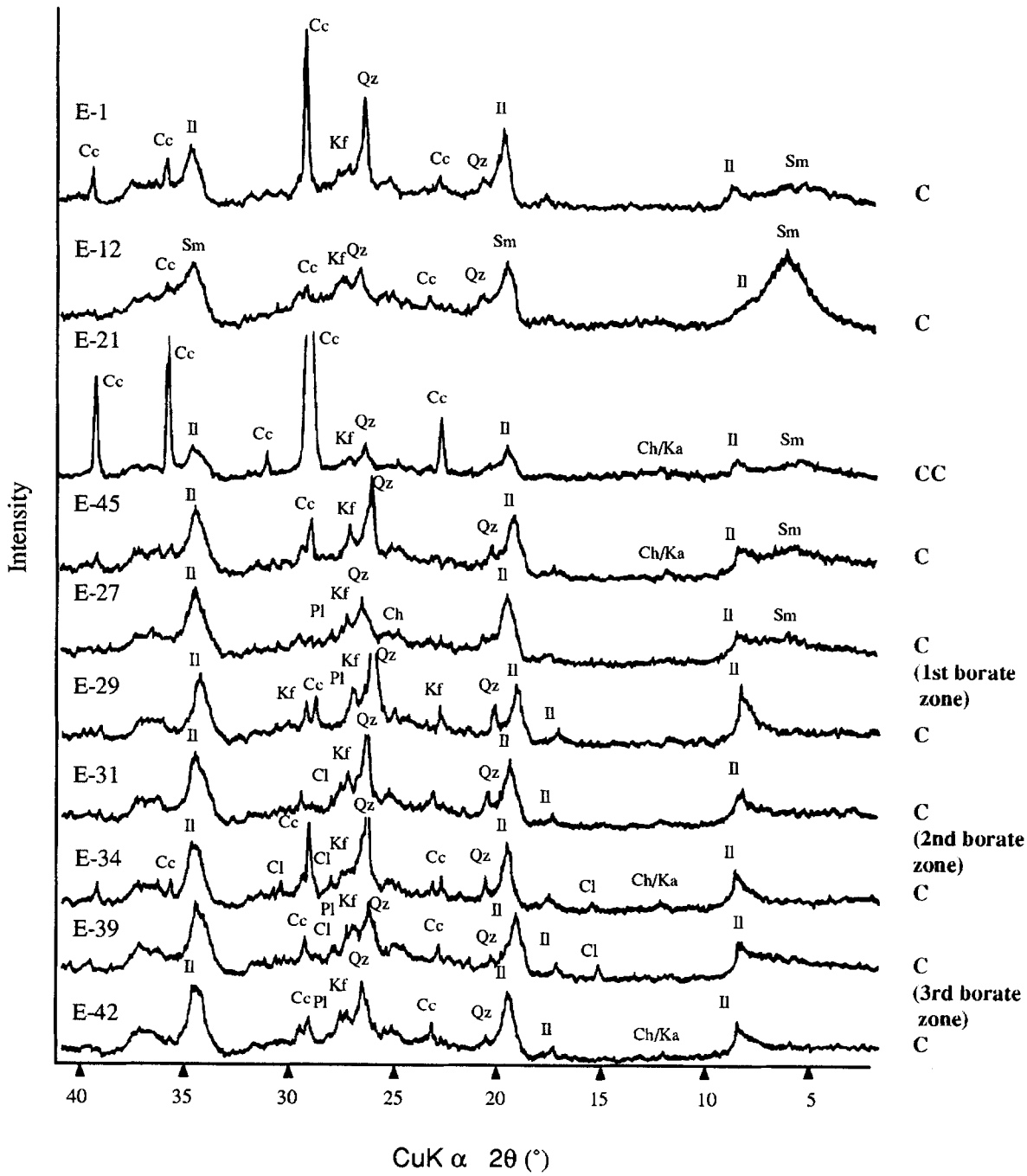

Figure 5. X-ray diffraction patterns of selected bulk samples from the Esbey colemanite open pit mine. (Cc: calcite, Qz: quartz, Kf: K-rich feldspar, Ca: cahnite, Pl: plagioclase, Cl: colemanite, Sm: smectite, Il: illite, Ch: chlorite, Ka: kaolinite). C: clay, CC: calcareous clay. Vertical axis is intensity.

were dried at room temperature, coated with Au under vacuum conditions in an Ar atmosphere, and examined by scanning electron microscopy (SEM) (JEOL-JSM-840A). Chemical analyses were performed using a Philips PW 1400 X-ray spectrometer with a Cr anode. Boron was analysed by inductively coupled plasma optical emission spectrometry (ICP-OES). FeO contents were determined using the dipyridilic method (Lange and Vejdelek, 1980) and analyzed with a PHILIPS PYE Unicam PU 8650 spectrophotometer.

https://doi.org/10.1346/CCMN.2000.0480401 Published online by Cambridge University Press

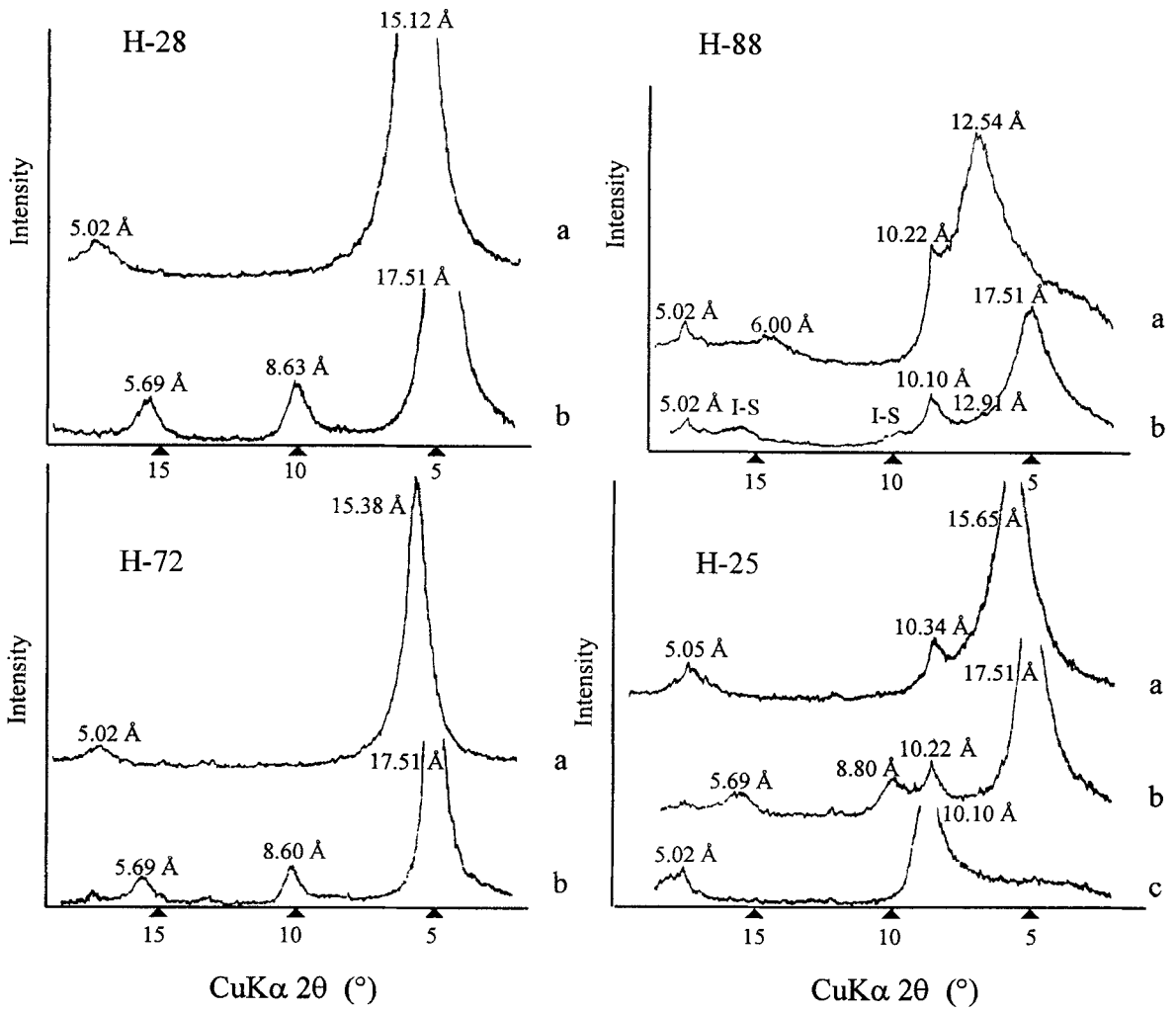

Figure 6. X-ray diffraction patterns in the <2-μm clay size fraction of select Hisarcık colemanite mine samples. Samples H-27, H-28, and H-39 were used for structural-formula calculations. The samples were not acid treated. Vertical axis is intensity.

The average error of the FeO analysis is ±0.02 wt. % based on reproducibility tests. The CO_2 and H_2O^+ contents were determined using a Leco RC-412 Multiphase carbon determinator. Grain sizes of the samples were analysed by a SediGraph-5100.

GEOLOGIC SETTING

In the Emet area, borate minerals occur in Neogene lacustrine sediments. These lacustrine sediments unconformably lie over Paleozoic metamorphic rocks consisting of marble, biotite schist, calcareous schist, and chlorite schist. The Neogene sequence consists of (1) a basal conglomerate and sandstone, (2) a lower limestone with thin layers of marl and tuff lenses, (3) a red unit forming strata of conglomerate, sandstone, clay, tuff, marl, and limestone, including coal and gypsum bands, (4) a borate-bearing unit of clay, tuff, and reworked tuff, and (5) an upper limestone unit with chert-marl and clay starata (Figure 1). The Paleocene Egrigöz granite, which is to the west of the study area, cuts the basement-rock units. Quaternary units consisting of terrace materials discordantly cover the Neogene sediments.

Volcanic activity began in the Emet area in the early Miocene and continued at least until late Miocene time. Volcanic rocks consist of a series of calc-alkaline flows (the earliest recorded lava flows are of rhyolites, dacites, and trachytes; the next lava flows are trachyandesitic-andesitic; and, finally, more recent flows are olivine-bearing andesitic basalts that are younger than the borate minerals) and abundant pyroclastic layers (Helvacı, 1984). The unit of clay, tuff, tuffite, and marl

https://doi.org/10.1346/CCMN.2000.0480401 Published online by Cambridge University Press

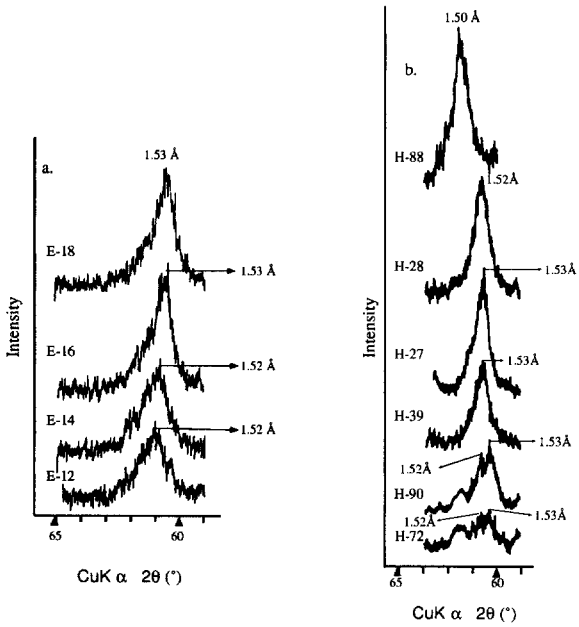

Figure 7. *d*(060) reflections of smectite samples from the (a) Esbey and (b) Hisarcık colemanite mine, (<2 μm, air-dried, non-oriented aggregates). Vertical axis is intensity.

containing the borate deposits has abundant realgar and orpiment in some horizons, indicating that arsenic and boron have a genetic volcanic relationship (Helvacı, 1984).

RESULTS

Lithology

Hisarcık. In the profile of the open-pit mine, "first-quality colemanite lower and upper zones" and "second-quality colemanite lower and upper zones" were defined by the engineers of the Etibank Mining Company to simplify the mining of the borate zones. The first-quality colemanite upper zone shows a transition to clay, calcareous clay, and limestone. The clays involved in the borate zone are between olive gray and dark olive brown in color. Fine-grained reworked tuffs usually are a light gray to olive gray color. Protonodules of colemanite with a lutitic matrix are common in the clay bands alternating with nodular colemanite layers. In addition, bioturbation is observed in reworked tuffs and calcareous clay layers in this deposit.

Bioturbation related to root growth is a common feature in mudflats of recent saline-lake environments (Hammer, 1986). At Hisarcık, the bioturbation traces are associated with bush plants or/and grasses, probably growing in an arid or semi-arid boron-free environment. The cylinder root tubes are dominantly vertical. The length of bioturbation is between 1–5 cm, and diameters vary from 0.5 to 2 mm. The filling of the tubes consists of massive (usually mottled) dark clay with variable amounts of orpiment and realgar.

Esbey. The first, second, and third borate zones were defined by engineers of the Etibank Mining Company. The upper limestones cover the borate zone. The thick bedded cream-colored limestone is overlain by olive gray-colored clay and calcareous clays. This clay and calcareous clay repetition increase towards the borate zone. Interbedded clays in the borate zone have colors between olive gray and dark green. Colemanite nodules have textures that are radial. The existence of clays both between the colemanite nodules and enveloping the nodules indicates that the clays were displaced during the growth of the colemanite nodules. Protonodules of colemanite rich in lutitic matrix are common in the clay bands that alternate with the nodular colemanite layers. Thin bedded, ferriginous altered reworked tuff (sample E-33) occurs below the second borate zone and is an important marker bed for the borate mining operation.

Whole-rock mineralogy

Hisarcık. The lithologic profile of the Hisarcık open-pit mine consists of fine-grained rocks, including marl, clay, and reworked tuffs. A summary of the mineralogy correlated to rock type is given in Table 1. The most important feature in Table 1 is that the arsenic minerals are common in the H-30 fine-grained tuff sample (Figure 4). Orpiment and realgar are rarely observed in colemanite nodules.

Calcite is the predominant mineral but no magnesian-containing mineral was found in any sample. Calcite varies from ~10 to ~30 wt. % in the clays interstratified with the colemanite nodules. However, the calcite ratio is from 1 to 5 wt. % in the reworked tuffs. Dolomite, which commonly replaces calcite in other sabkha environments, remarkably, is absent. The lack of dolomite results in elevated Mg^{2+}/Ca^{2+} molar ratios. High Mg^{2+} concentrations in the Hisarcık colemanite deposit may result in Mg-rich smectite formation. Secondary colemanite (Figure 4) is the main mineral after calcite in the clay-rich samples which form in fractures. Realgar preserves its original red color in the clay layers. The H-41 sample contains abundant orpiment, and it has yellowish color. Celestite occurs in the center of the nodular colemanite and in clay layers (H-53 and H-76). Cristobalite is present in the clay samples (Figure 4) occurring in the upper limestones. Cristobalite has a broad (111) reflection at 4.14 Å.

Esbey. Whole-rock mineralogy is given in Table 1. Calcite is also the main mineral in the Esbey colemanite mine. The calcite in calcareous clays varies between 25–65 wt. %. The interstratified clay layers and clays associated with the colemanite nodules have 5 and 1–2 wt. % calcite, respectively. Quartz, K-rich feldspar, plagioclase, cahnite, colemanite, and clay minerals are present.

https://doi.org/10.1346/CCMN.2000.0480401 Published online by Cambridge University Press

Table 2. Major (wt. %) oxide analyses of the Hisarcık colemanite mine samples (given in stratigraphical order).

Sample number	SiO_2	TiO_2	Al_2O_3	Fe_2O_3	FeO	MnO	MgO	CaO	Na_2O	K_2O	P_2O_5	B_2O_3	H_2O^+	CO_2	Total
H-89	46.16	0.49	13.90	2.98	0.27	0.03	2.98	13.72	0.18	3.01	0.27	n.a	5.92	10.38	100.29
H-88	64.14	0.58	13.36	3.34	0.21	0.02	2.96	4.31	0.19	2.91	0.43	n.a	6.37	0.99	99.80
H-87	56.52	0.44	13.38	2.93	0.26	0.02	3.05	8.49	0.20	2.76	0.54	n.a	6.10	5.39	100.08
H-1	57.77	0.68	14.42	6.19	0.78	0.04	3.63	1.72	0.31	7.49	0.11	n.a	5.75	1.02	99.91
H-3	47.41	0.51	11.64	4.86	0.57	0.04	2.88	12.89	0.20	6.02	0.26	n.a	5.08	8.06	100.42
H-6	58.09	0.66	13.76	4.48	0.34	0.02	4.50	2.43	0.32	6.02	0.15	n.a	7.14	2.15	100.06
H-10	50.09	0.23	5.27	1.67	0.31	0.02	17.39	7.52	0.10	1.91	0.13	n.a	9.47	5.83	99.94
H-13	31.50	0.27	5.87	1.45	0.44	0.04	7.40	25.04	0.15	3.37	0.11	n.a	4.13	20.17	99.94
H-14	40.28	0.14	3.30	0.80	0.36	0.03	15.46	17.08	0.04	1.48	0.07	n.a	6.38	14.49	99.91
H-16	55.10	0.29	6.25	2.45	0.40	0.02	18.10	3.95	0.04	2.99	0.19	n.a	7.40	3.26	100.44
H-20	50.50	0.31	8.18	2.17	0.36	0.07	14.14	7.88	0.10	4.55	0.19	n.a	5.75	6.27	100.47
H-21[1]	46.47	0.37	11.02	1.75	0.34	0.04	5.85	12.69	0.13	7.92	0.11	n.a	3.37	10.01	100.07
H-22	34.30	0.17	3.69	1.17	0.36	0.06	12.44	22.90	0.08	1.56	0.15	n.a	4.90	18.41	100.19
H-24	52.98	0.13	2.92	0.83	0.48	0.03	23.90	5.01	0.04	0.86	0.16	n.a	7.33	5.10	99.77
H-25	40.89	0.36	7.53	1.85	0.72	0.08	11.57	13.65	0.12	3.95	0.22	n.a	4.98	13.68	99.60
H-38[1]	35.72	0.37	8.49	1.27	0.78	0.08	7.36	18.71	0.16	4.97	0.12	n.a	3.58	15.26	96.87
H-36	51.33	0.21	4.33	1.74	0.76	0.03	24.08	3.40	0.04	0.92	0.13	n.a	8.43	4.11	99.51
H-34	50.45	0.17	3.94	1.22	0.57	0.04	24.93	4.95	0.18	0.56	0.11	n.a	8.36	4.51	99.99
H-33[1]	47.70	0.38	8.97	2.32	3.09	0.05	22.87	2.11	0.05	1.50	0.10	n.a	9.17	1.15	99.46
H-32[1]	37.52	0.56	11.08	1.95	3.27	0.12	15.93	10.92	0.07	2.72	0.21	n.a	7.58	8.14	100.07
H-30[1]	41.80	0.16	10.56	0.75	2.03	0.02	29.16	1.64	0.04	0.14	0.02	n.a	10.40	0.69	97.41
H-29	44.50	0.14	2.74	0.34	0.61	0.08	23.03	9.91	0.04	0.28	0.04	2.62	7.48	8.16	99.47
H-85	41.93	0.15	11.41	1.10	2.58	0.02	29.54	1.58	0.04	0.18	0.02	n.a	10.70	0.66	99.92
H-28	50.05	0.15	2.84	0.55	0.43	0.03	25.10	5.20	0.04	0.41	0.06	0.37	10.70	4.80	100.73
H-39	24.91	0.05	1.25	0.09	0.38	0.06	13.00	28.15	0.03	0.13	0.08	1.86	4.93	23.38	98.30
H-40	53.24	0.07	1.46	0.25	0.39	0.02	26.07	3.49	0.04	0.26	0.12	n.a	7.60	4.84	97.85
H-41[1]	45.01	0.15	3.28	0.69	0.41	0.03	23.07	6.88	0.05	0.41	0.25	n.a	6.59	1.73	88.55
H-42	44.86	0.24	5.28	0.90	1.13	0.05	22.49	7.39	0.04	0.67	0.11	n.a	8.27	6.86	98.29
H-43	52.77	0.19	4.65	0.90	0.79	0.04	25.28	2.44	0.04	0.84	0.05	n.a	8.44	3.35	99.78
H-44[1]	45.15	0.38	9.93	2.40	1.05	0.07	12.92	9.14	0.09	5.03	0.10	n.a	5.91	7.19	99.36
H-45	54.49	0.10	3.36	0.29	0.46	0.02	26.91	2.59	0.04	0.29	0.15	n.a	8.51	3.19	100.40
H-86[1]	50.07	0.10	13.32	0.20	1.01	0.01	3.88	5.22	0.22	10.84	0.01	9.45	5.29	0.31	99.93
H-46	52.56	0.20	4.22	0.83	0.86	0.03	25.47	2.44	0.04	0.77	0.25	0.37	8.22	2.88	99.14
H-48	52.30	0.19	4.99	0.93	0.97	0.03	22.33	2.01	0.04	1.86	0.21	n.a	9.36	4.25	99.47
H-49[1]	56.00	0.46	13.58	1.28	1.54	0.03	11.01	1.38	0.16	8.73	0.06	n.a	4.88	0.54	99.65
H-50	52.40	0.47	11.77	2.10	1.31	0.05	12.66	2.63	0.09	6.76	0.16	0.39	6.02	1.67	98.48
H-51	52.95	0.17	7.16	1.12	1.00	0.03	20.14	1.81	0.05	3.11	0.04	n.a	7.21	2.23	97.02
H-52[1]	62.76	0.10	16.66	0.24	0.68	0.01	2.43	0.28	0.17	14.58	0.01	n.a	1.37	0.23	99.52
H-53	45.41	0.17	5.28	0.98	0.90	0.03	20.04	2.12	0.05	1.34	0.07	n.a	6.56	2.15	85.10
H-55	50.60	0.14	5.57	1.03	0.72	0.04	21.28	5.31	0.04	1.91	0.03	n.a	7.16	4.22	98.05
H-56	38.09	0.13	4.00	1.50	0.60	0.05	17.54	11.94	0.04	0.98	0.05	n.a	5.91	10.86	91.69
H-58	47.40	0.46	11.07	2.04	1.00	0.03	6.57	9.08	0.11	7.67	0.21	n.a	3.67	9.39	98.70
H-61	51.44	0.13	3.80	0.86	0.97	0.03	24.89	2.59	0.04	0.43	0.14	n.a	7.20	3.99	96.51
H-63[1]	47.22	0.51	10.69	1.26	1.01	0.03	5.35	11.73	0.19	7.70	0.04	n.a	3.26	11.30	100.29
H-65	49.89	0.24	6.63	2.03	1.25	0.04	19.15	3.93	0.04	2.93	0.10	n.a	6.32	4.47	97.02
H-67	50.10	0.22	6.77	3.22	1.46	0.04	18.25	2.03	0.06	3.14	0.17	0.31	6.28	3.07	95.12
H-68[1]	57.71	0.62	13.46	1.89	1.34	0.05	7.74	1.92	0.20	8.73	0.07	n.a	4.40	1.60	99.73
H-69	54.38	0.31	9.28	2.14	1.66	0.04	15.75	2.22	0.08	5.34	0.11	n.a	5.75	3.04	100.10
H-71[1]	57.11	0.36	11.14	2.23	0.95	0.06	12.84	1.70	0.12	6.46	0.16	n.a	5.60	1.38	100.11
H-72[1]	61.39	0.20	12.97	1.33	0.40	0.02	8.28	1.09	0.18	9.51	0.03	n.a	4.03	0.42	99.85
H-73	42.00	0.13	3.84	0.70	0.97	0.08	16.94	7.06	0.04	1.68	0.10	6.79	7.35	5.94	93.62
H-90[1]	61.98	0.09	15.00	0.16	0.14	0.01	6.17	0.59	0.22	12.39	0.01	n.a	3.02	0.36	100.12
H-74	52.81	0.37	11.16	2.19	1.51	0.06	11.58	3.71	0.09	6.28	0.12	n.a	5.08	3.53	98.49
H-76	42.05	0.44	9.90	2.75	1.06	0.04	9.03	5.13	0.40	4.97	0.22	12.98	8.03	1.42	98.42
H-77[1]	53.30	0.62	14.26	3.02	1.64	0.06	9.22	2.71	0.19	7.88	0.15	n.a	5.22	1.64	99.91

[1] Reworked tuffs, analyst: M. Çolak, Institute of Mineralogy and Petrography, Fribourg-Switzerland.

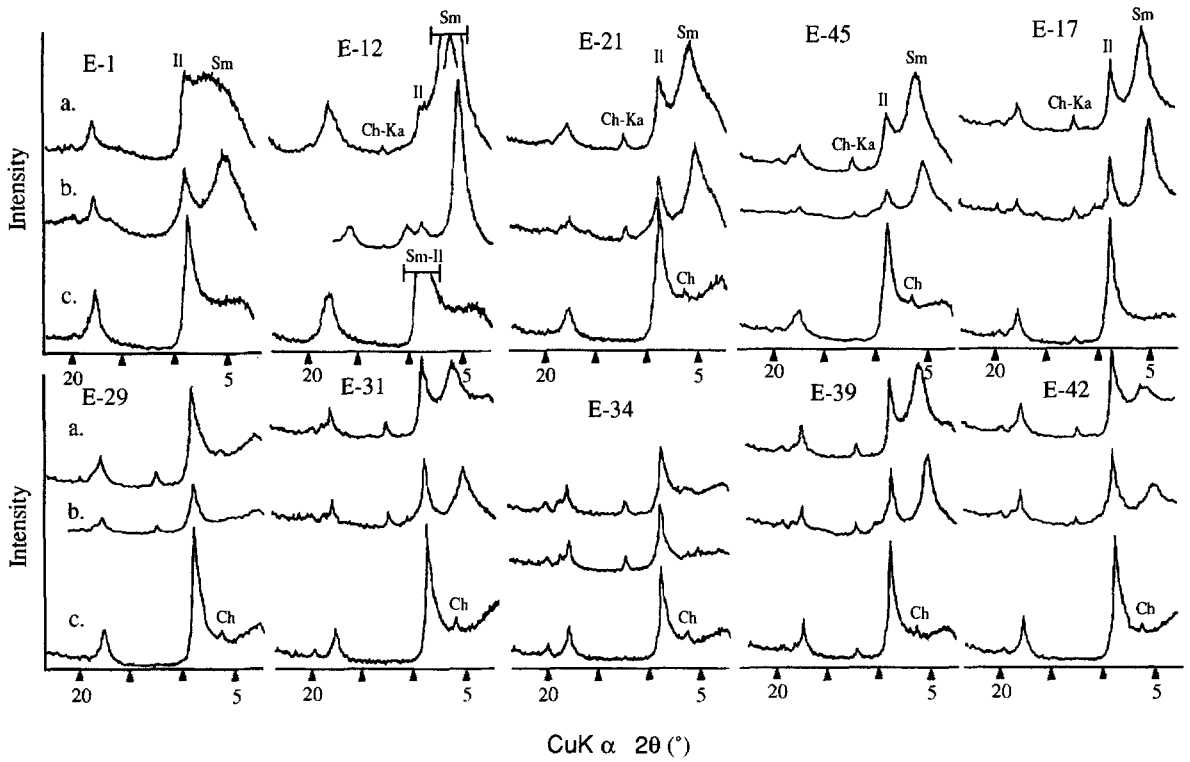

Figure 8. X-ray diffraction patterns of selected clay samples (<2 μm) from the Esbey colemanite mine. Abbreviations: Sm: smectite, Il: illite, Ch: chlorite, Ka: kaolinite. Pattern a: air-dried, b: glycolated, c: heated at 550°C. Vertical axis is intensity.

Cahnite (Figure 5) is the other important arsenic-bearing borate mineral. Magnesium-bearing minerals do not occur, except for Mg-rich smectite.

Clay minerals

Hisarcık. XRD patterns indicate that smectite and illite clay minerals are present (Figure 6) in approximately equal amounts in the clay layers interstratified with upper limestones in the open-pit-mine profile. I-S containing 70% illite and 30% smectite (I_{70}-S) interstratified clay was determined to be between 2–4 wt. % in the clay fraction. In the first-quality colemanite upper zone, smectite is dominant at 70–100 wt. % in the clay fraction and especially high in samples H-8, H-23, and H-29. Illite occurs at 50–70 wt. % in the clay strata proximate to the upper limestones, whereas only 5–12 wt. % in the reworked tuffs. In some samples, between 2–6 wt. % of chlorite and between 2–3 wt. % of kaolinite were found (Figure 2). Smectite is the major clay mineral in the second-quality colemanite upper zone with 60–90 wt. % present. Samples H-72 and H-90, which are reworked tuffs, have 100 wt. % smectite in the clay fraction. In this zone, the amount of illite increases towards the bottom in the range of between 25–40 wt. %. Chlorite occurs at 2–5 wt. %. The smectite content of the clays is highest in the colemanite upper zone. Illite content increases towards the lower parts of the profile, although it is also present in considerable amounts in the upper limestone portion.

The clay fraction of samples H-27, H-28, H-72, H-88, and H-90, which contain high amounts of smectite, were examined. The d(001) reflections of smectites are at 14 Å under ambiant conditions and at ~17 Å after saturation with ethylene glycol. The d(060)-reflection value (Figure 7) is >1.51 Å in all samples except H-88, indicating that the smectite in all but H-88 is close to trioctahedral.

Clay sample H-88, which is intrastratified with upper limestones, contains 52 wt. % smectite, 43 wt. % illite, and 4 wt. % I_{70}-S. The 002/003 reflection of illite-smectite in sample H-88 is broad (Figure 6). There is some uncertainty concerning I-S in the diffraction pattern of glycolated material, but if present, it is very low and occurs only in samples H-87, H-88, and H-89. The peak position of I-S changes from 15.2 Å (a smectite-like interlayer) to 10 Å (an illite-like interlayer) depending on smectite content in the air-dried state (Velde, 1992). The strong reflection at 12.5 Å (in the air-dried state) indicates interstatification of I-S (Figure 6). An illite XRD peak at d(060) = 1.50 Å was not observed, although a d(060) reflection at 1.50 Å is believed to belong to dioctahedral smectite. Samples containing mostly smectite, H-72, and H-90

https://doi.org/10.1346/CCMN.2000.0480401 Published online by Cambridge University Press

Table 3. Smectite and smectite-illite analyses (wt. %). Samples are from the <2-μm size fraction. Illite is present in samples E-12, E-14, E-16, and E-18, whereas samples H-27, H-28, and H-39 are believed to be pure or nearly pure smectite.

Sample number	SiO_2	TiO_2	Al_2O_3	Fe_2O_3	FeO	MnO	MgO	CaO	Na_2O	K_2O	Li_2O	H_2O^+	Total
H-27	58.49	0.10	2.77	0.02	0.92	0.12	30.17	0.00	0.08	0.23	n.a	6.92	99.82
H-28	57.80	0.18	3.41	0.57	0.54	0.04	29.28	1.95	0.22	0.77	0.58	3.98	99.32
H-39	60.50	0.12	3.18	0.53	0.64	0.07	30.33	0.00	0.07	0.22	0.56	3.59	99.81
E-12	61.77	0.34	7.97	2.74	0.24	0.03	20.15	0.86	0.10	2.12	n.a	3.67	99.99
E-14	63.31	0.30	7.01	2.80	0.32	0.03	22.23	0.01	0.05	2.11	0.60	1.18	99.95
E-16	55.22	0.30	8.42	3.57	0.34	0.03	21.96	0.47	0.08	1.65	n.a	7.92	99.96
E-18	52.84	0.29	8.25	4.51	0.28	0.03	22.55	1.47	0.04	1.38	0.24	7.86	99.74

show XRD peaks at $d(060)$ = 1.50 Å, indicating a transition of dioctahedral to trioctahedral smectite.

Illite was found only in small quantities in the Hisarcık colemanite mine, although samples H-4 and H-6 contained sufficient illite (62 and 76 wt. % illite, respectively) to determine polytype content. The $1M/2M_1$ ratios are 0.11 for H-4 and 0.13 for H-6.

Esbey. The composition of the clay fraction (<2 μm) is similar but varies slightly between the uppermost, upper, and bottom zones at Esbey (Figure 3). The uppermost zone (above sample E-12 in Figure 3) contains illite at 35–75 wt. %, smectite at 20–55 wt. %, and minor chlorite. The upper zone (only E-12) has abundant smectite at 40–90 wt. %, illite at 16–40 wt. %, and chlorite and kaolinite are minor. The borate-bearing bottom zone is dominated by illite at 30–85 wt. %, followed by smectite at 20–60 wt. %. Chlorite and kaolinite are minor. Figure 8 shows X-ray diffraction patterns of selected samples from the Esbey stratigraphic profile. XRD intensities of smectite are lower in samples from the bottom portion of the profile.

The clay fraction of sample E-12, E-14, E-16, and E-18 contains high amounts of smectite. The $d(060)$-reflection position is >1.51 Å, suggesting a smectite end-member that is trioctahedral (Figure 7).

Illite is an abundant mineral in this mine. High illite content in the clay strata alternating with borate-rich strata may be related (1) to the rapid transformation of smectite to illite or (2) to the transport of (detrital) illite into the region. The polytype analysis of illite shows that the $2M_1$ polytype is common in samples E-19, E-21, E-29, E-33, and E-42 (each >11%) and suggests a detrital component in both the calcareous and tuffite samples. A high percentage of $2M_1$-illite polytype was observed in calcareous clay. The tuffite sam-

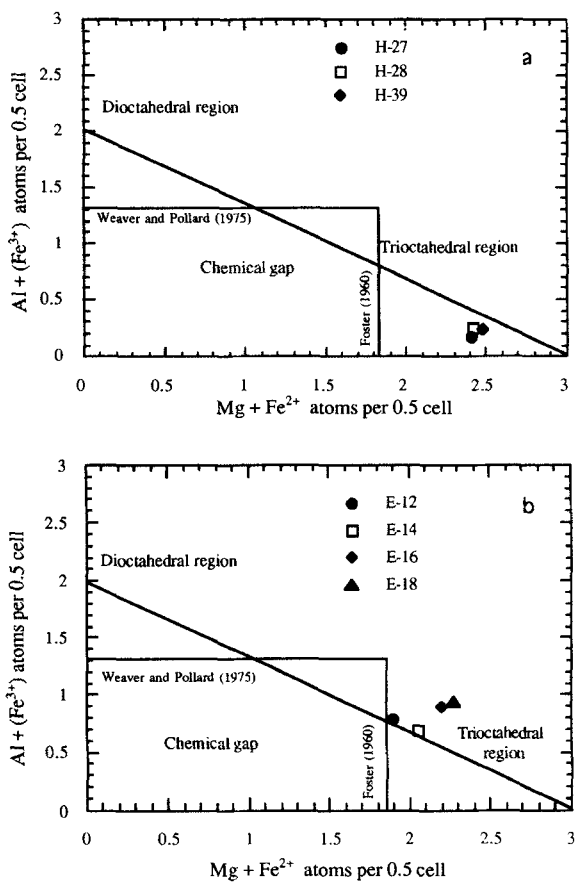

Figure 9. Octahedral composition of the (a) Esbey and (b) Hisarcık smectites according to Mg + Fe^{2+} atoms per 0.5 cell *versus* Al + (Fe^{3+} <0.4) atoms per 0.5 cell (after Grauby *et al.*, 1993).

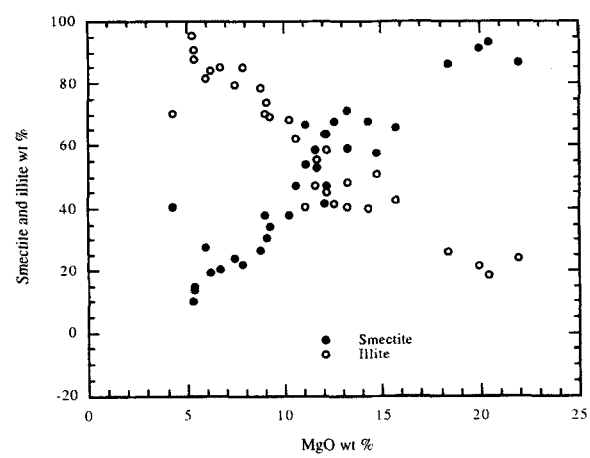

Figure 10. Variation of smectite and illite percentage in the <2-μm fraction of the Esbey colemanite mine.

https://doi.org/10.1346/CCMN.2000.0480401 Published online by Cambridge University Press

Table 4. Major (wt. %) element analyses of the Esbey colemanite mine samples (given in stratigraphical order).

Sample number	SiO_2	TiO_2	Al_2O_3	Fe_2O_3	FeO	MnO	MgO	CaO	Na_2O	K_2O	P_2O_5	B_2O_3	H_2O^+	CO_2	Total
E-1	51.81	0.70	16.32	4.04	0.40	0.04	4.37	7.65	0.18	3.69	0.26	n.a	5.31	5.25	100.02
E-2	28.34	0.36	7.95	2.03	0.35	0.04	2.51	29.85	0.14	1.82	0.12	n.a	2.62	23.24	99.37
E-6	43.06	0.41	8.93	2.46	0.49	0.04	10.00	15.28	0.24	2.61	0.15	n.a	4.46	11.63	99.76
E-9	46.76	0.65	13.79	3.81	0.69	0.05	5.84	12.50	0.50	4.00	0.32	n.a	3.90	7.51	100.32
E-8	17.87	0.25	5.09	1.08	0.54	0.03	2.99	37.61	0.21	1.29	0.11	n.a	2.19	30.73	99.99
E-10	57.05	0.57	12.60	3.36	0.59	0.04	13.28	2.05	0.26	3.60	0.07	n.a	5.73	0.91	100.11
E-12	57.64	0.39	8.24	2.56	0.35	0.03	18.04	2.28	0.11	2.27	0.05	n.a	6.16	1.16	99.28
E-14	56.31	0.34	6.72	2.40	0.41	0.03	19.43	3.55	0.08	2.13	0.08	n.a	6.15	2.39	100.02
E-16	48.39	0.33	7.78	3.18	0.50	0.04	19.25	7.38	0.04	1.48	0.05	n.a	6.44	5.06	99.92
E-17	19.40	0.18	4.13	1.17	0.46	0.05	7.88	34.33	0.03	0.87	0.11	n.a	2.95	28.42	99.98
E-18	50.55	0.36	8.45	3.83	0.52	0.04	21.25	4.02	0.06	1.55	0.23	n.a	7.09	1.99	99.94
E-19	41.57	0.54	11.94	4.11	0.72	0.06	10.27	13.09	0.10	2.92	0.22	n.a	5.69	9.20	100.43
E-21	22.21	0.31	6.63	2.28	0.35	0.03	5.02	31.91	0.05	1.85	0.18	n.a	3.36	25.23	99.41
E-22	52.80	0.53	12.01	4.50	0.58	0.15	15.55	2.62	0.12	3.33	0.29	n.a	6.92	1.09	100.49
E-45	49.80	0.60	13.27	4.42	0.80	0.09	11.09	4.61	0.18	3.93	0.25	n.a	8.06	2.89	99.99
E-46	50.67	0.54	13.42	4.48	0.72	0.07	12.13	2.93	0.17	4.00	0.28	n.a	8.92	1.42	99.75
E-23	21.18	0.15	3.28	1.01	0.36	0.04	9.88	28.26	0.04	0.76	0.05	2.99	5.11	20.82	93.93
E-24	50.93	0.59	13.34	4.89	0.68	0.10	14.48	2.59	0.14	3.68	0.35	n.a	7.20	0.73	99.70
E-25	52.12	0.72	16.27	5.39	0.77	0.08	9.33	1.97	0.21	5.13	0.26	n.a	7.16	0.41	99.82
E-27	50.04	0.64	14.47	5.47	0.83	0.11	11.89	2.97	0.22	4.36	0.41	1.78	6.65	0.62	100.46
E-28	50.77	0.70	15.88	5.40	1.07	0.11	6.15	3.60	0.37	5.76	0.26	n.a	6.98	0.57	97.62
E-29	51.56	0.71	15.32	4.97	1.34	0.12	5.42	3.47	0.35	6.81	0.24	2.88	5.94	1.09	100.22
E-30	53.53	0.51	10.11	3.62	2.74	0.11	13.95	1.76	0.14	4.16	0.13	n.a	5.49	3.97	100.22
E-31	53.17	0.66	14.43	4.62	1.26	0.11	9.06	2.39	0.38	5.38	0.38	1.99	6.08	0.80	100.71
E-32	52.87	0.71	15.55	4.92	1.42	0.11	6.85	2.71	0.48	6.41	0.26	n.a	5.83	0.98	99.10
E-33[1]	55.18	0.59	15.31	2.41	2.54	0.05	2.38	2.69	0.49	12.08	0.20	n.a	2.66	0.13	96.71
E-34	43.09	0.57	13.65	4.35	1.12	0.12	4.70	4.41	0.34	5.34	0.20	n.a	5.78	2.68	86.35
E-35	47.18	0.64	15.37	4.73	1.21	0.20	5.26	7.81	0.36	6.00	0.21	n.a	4.88	5.84	99.69
E-36	53.40	0.65	15.33	5.09	1.24	0.12	8.91	1.88	0.48	5.66	0.30	n.a	6.32	0.70	100.08
E-37	49.62	0.68	14.87	5.02	0.94	0.12	7.24	3.59	0.52	5.76	0.31	4.77	6.83	0.45	100.72
E-38	55.18	0.66	15.45	5.25	1.16	0.10	12.35	1.96	0.47	5.47	0.32	n.a	0.75	0.59	99.71
E-39	47.96	0.59	14.15	3.85	1.39	0.09	9.58	2.78	0.38	4.99	0.26	7.41	5.96	0.62	100.01
E-40	52.79	0.55	12.88	3.53	1.29	0.09	13.09	1.86	0.26	5.44	0.31	0.54	5.71	2.16	100.50
E-41	43.92	0.50	12.12	3.69	1.01	0.15	10.37	9.98	0.37	4.24	0.20	n.a	4.97	7.59	99.11
E-48	51.45	0.61	14.74	4.62	0.92	0.10	10.28	1.70	0.45	4.91	0.22	n.a	8.72	0.82	99.54
E-47	50.86	0.54	13.42	5.14	0.32	0.11	11.76	1.99	0.32	5.20	0.29	0.55	6.85	2.01	99.39
E-42	53.48	0.64	16.75	4.52	1.26	0.10	8.04	2.20	0.36	6.26	0.21	n.a	5.48	1.08	100.38

[1] Reworked tuff, analyst: M. Çolak, Institute of Mineralogy and Petrography, Fribourg-Switzerland.

ple has also a high percentage of the 1*M*-illite polytype.

Smectite chemistry

Hisarcık. The whole-rock chemical analyses (Table 2) showed that samples contain 10–29.54 wt. % of MgO. Because no other Mg-rich mineral was detected by XRD, the magnesium is probably bound in the clay minerals. Chemical analysis of samples H-28, H-27, and H-39, which are rich in smectite, are shown in Table 3. Compared to hectorite, samples H-28 and H-39 have a high content of Al^{3+} and Fe^{3+}. Compared to stevensite, sample H-27 has higher Al^{3+} and Fe^{3+} concentrations. Lithium is present at 0.58 wt. % in sample H-28 and at 0.56 wt. % in sample H-39. Thus, these results indicate that Hisarcık smectites are Li-bearing saponite.

The samples of the clay fractions always include calcite. The carbonate contamination of samples may lead to an aggregation of clay particles when sample suspensions are reacted with HCl before analysis. However, the sensitivity of trioctahedral smectites to HCl prevented this from occurring. The calcite content was calculated on the basis of CO_2 analyses. Structural formulae for smectite are determined as: H-27, $(Na_{0.02}, K_{0.04})(Mg_{5.87}, Al_{0.07}, Fe^{2+}_{0.1})(Si_{7.64}, Al_{0.36})O_{20}(OH)_4$; H-28, $(Ca_{0.27}, Na_{0.06}, K_{0.13})(Mg_{5.62}, Li_{0.30}, Fe^{3+}_{0.06}, Fe^{2+}_{0.06}, Ti_{0.02})(Si_{7.44}, Al_{0.52})O_{20}(OH)_4$; H-39, $(Na_{0.02}, K_{0.04})(Mg_{5.69}, Al_{0.08}, Li_{0.28}, Fe^{3+}_{0.05}, Fe^{2+}_{0.07}, Ti_{0.01})(Si_{7.61}, Al_{0.39})O_{20}(OH)_4$.

Grauby *et al.* (1993), Weaver and Pollard (1975), and Foster (1960) considered the octahedral content of smectite in the classification of smectites. Weaver and Pollard (1975) placed limits on dioctahedral smectites (to 1.3 R^{3+} cation limits) and Foster (1960) limited trioctahedral smectites (to 1.83 R^{2+} cation limits) (see Figure 9). Grauby *et al.* (1993) noted that few chemical analyses of natural smectites fall outside this chemical range. The chemistry of the Hisarcık smectites plots in or near the trioctahedral region, which is consistent with this earlier work.

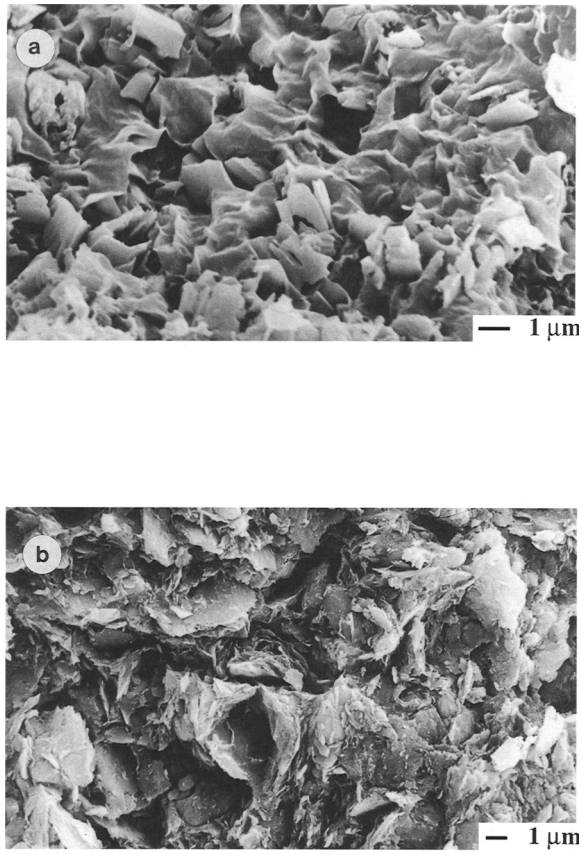

Figure 11. SEM image of clays: (a) wavy flakes of smectite with calcite in sample H-51 from the Hisarcık colemanite mine, (b) smectite showing large flakes and blocky morphology in sample E-29 from the Esbey colemanite mine.

Esbey. The results of the whole-rock analyses (Table 4) showed that samples contain between 4.70–21.25 wt. % of MgO. Similar to Hisarcık samples, smectite is the only mineral containing significant magnesium. In Figure 10, smectite and illite content in the clay fraction was plotted against the MgO content of the bulk analysis of the calcareous clay and clay samples. Smectite was positively correlated and illite was negatively correlated to the MgO concentration.

The Esbey clay fraction is inhomogeneous and contains illite (10–15 wt. %) and chlorite and kaolinite (1–3 wt. %). Therefore, these analyses do not represent the chemical composition of the smectite. The high K_2O, Fe_2O_3, and Al_2O_3 content of the Esbey clay fraction suggests small amounts of impurity. The analyses of the Esbey clay fraction are given in Table 3. If Al_2O_3 and Fe_2O_3 are assumed to be related to K-rich illite, the remaining Al_2O_3 and Fe_2O_3 suggest the existence of saponite. The lithium content for samples E-14 and E-18 is 0.60 and 0.24 wt. %, respectively, which further suggests that the Esbey smectite is a lithium-bearing saponite. The trioctahedral character is illustrated in the plot of Figure 9.

SEM studies

SEM photographs (Figure 11) show that the smectite has a wavy appearance. Calcite crystals accompanied the smectite in the Hisarcık sample. Dissolution and precipitation processes result in a honeycomb structure for smectite growth (Henning and Störr, 1986).

DISCUSSION

Origin of saponite

Smectites may form by the weathering of mafic or felsic igneous rocks (Harder, 1972) and the composition of the parent rock, such as the alkali and magnesium content, influences the product phases. From mafic rocks with high magnesium content, smectite formation is possible under basic conditions, but if the parent material is felsic glass then smectite may form in neutral pH conditions. From felsic magmatic rocks with a low content of magnesium, smectite formation is only possible under basic pH conditions.

The borate deposits show variable concentrations of Mg, Sr, and As. The presence of realgar, orpiment, elemental sulfur, and veachit-A supports a volcanic origin for As, Sr, and B (Helvacı and Orti, 1998). Kistler and Helvacı (1994) postulated that ions in solution that occur in the basins were supplied by the leaching of Tertiary volcanic rocks (enriched with B and Sr) and basement metamorphic rocks. Transport to the basins was by thermal springs and hydrothermal solutions associated with the volcanism. The Emet borate deposits (Helvacı and Firman, 1976) are characterized by colemanite, very low Na, and relatively high Mg, Sr, As, and S concentrations. The Mg, Sr, As, and S are present both in the evaporite and in the clay fractions, but mainly in the latter. During diagenesis, some of these elements were probably incorporated in the borate minerals by base exchange, resulting in the formation of various borate and non-borate minerals such as hyroboracite, veachit-A, and cahnite (Helvacı, 1977).

Helvacı (1984) showed that secondary alterations play an important role in modifying the chemistry of the Emet basin. For example, colemanite reacting to hydroboracite, veachit-A, and cahnite illustrates this process. Most of the clay minerals in the Emet deposits were formed by the weathering of pyroclastic material. During this process, magnesium was added, and magnesium-rich waters probably moved through the reworked tuff and clay (mud-flat) strata. A high MgO content was determined in the Hisarcık and Esbey colemanite samples, especially in associated clay layers. This high MgO content decreases in the reworked tuff layers, although they are interbedded with MgO-rich clay. The presence of K^+ as the dominant interlayer cation in smectite is common in hypersaline environments (Hover *et al.*, 1999). However, there is a near negative correlation between MgO and K_2O con-

https://doi.org/10.1346/CCMN.2000.0480401 Published online by Cambridge University Press

centrations in the Hisarcık colemanite deposit. K^+ mostly depends on the illite concentration of samples. Trace element analyses (not included here) show high Sr and As contents in the borate zone. However, there is no apparent relationship between MgO, Sr, and As.

Precipitation of Mg-rich trioctahedral saponite on original detrital smectite and/or neoformed dioctahedral smectite may explain the wide range of Mg/Al ratios and the apparent complex solid-solution between di- and trioctahedral components. We suggest that the smectites alter from dioctahedral to trioctahedral smectites with increasing salinity.

ACKNOWLEDGMENTS

This work was partly supported by a grant from Dokuz Eylül University. We thank the Directorate of Etibank Mining Company, Emet Colemanite Enterprise, G. Kahr of ETH-Zurich, M. Schwikowski of the Paul Scherrer Institute, and T. Hustings of Micromeritics. We thank G. Austin, N. O'Brien, and an anonymous referee for their reviews and constructive criticism of the manuscript. We are also grateful to S. Guggenheim and W.D. Huff for reviewing the manuscript and making many valuable comments and suggestions.

REFERENCES

Ataman, G., and Baysal, O. (1978) Clay mineralogy of Turkish borate deposits. *Chemical Geology,* **22,** 233–247.

Dündar, A., Güngör, N., Gürsel, T., Özden, M., and Özyeğin, E. (1986) *Kütahya-Emet bor tuzu yatağı nihai değerlendirme raporu.* Mineral Research and Exploration Institute of Turkey (MTA) Report, Ankara, 151 pp.

Foster, M. (1960) *Interpretation of the composition of trioctahedral micas.* U.S. Geological Survey Professional Paper 354 B, Washington, D.C., 11–43.

Gibbs, R.S. (1965) Error due to segregation in quantitative clay mineral X-ray diffraction mounting techniques. *American Mineralogist,* **50,** 741–751.

Gibbs, R.S. (1968) Clay mineral mounting techniques for X-ray diffraction analysis. A discussion. *Journal of Sedimentary Petrology,* **38,** 242–244.

Grauby, O., Petit, S., Decarreau, A., and Baronnet, A. (1993) The beidellite-saponite series: An experimental approach. *European Journal of Mineralogy,* **5,** 623–635.

Hammer, U.T. (1986) *Saline Lake Ecosystems of the World.* Junk, Dordrecht, 616 pp.

Harder, H. (1972) The role of magnesium in the formation of smectite minerals. *Chemical Geology,* **10,** 31–39.

Helvacı, C. (1977) Geology, mineralogy and geochemistry of the borate deposits and associated rocks at the Emet valley, Turkey. Ph.D. thesis, University of Nottingham, U.K., 338 pp.

Helvacı, C. (1983) Türkiye Borat Yataklarının Mineralojisi. *Jeoloji Mühendisliği Dergisi,* Mayıs, 37–54.

Helvacı, C. (1984) Occurence of rare borate minerals: Veatchit-A, Tunellite, Teruggite and Cahnite in the Emet borate deposits, Turkey. *Mineral Deposita,* **19,** 217–226.

Helvacı, C. (1986) *Stratigraphic and Structural Evolution of the Emet Borate Deposits, Western Anatolia, Turkey.* Dokuz Eylül University, İzmir, Turkey, Research Paper MM/JEO-86, 8, 28 pp.

Helvacı, C., and Firman, R.J. (1976) Geological setting and mineralogy of Emet borate deposits, Turkey. *Transactions, Institute of Mining and Metallurgy,* **85,** 142–152.

Helvacı, C., and Orti, F. (1998) Sedimentalogy and diagenesis of Miocene colemanite-ulexite deposits (Western Anatolia, Turkey). *Journal of Sedimentary Research,* **68,** 1021–1033.

Helvacı, C., Stamatakis, M.G., Zagouroglou, C., and Kanaris, J. (1993) Borate minerals and related authigenic silicates in northeastern Mediterranean Late Miocene Continental basins. *Exploration Mining Geology,* **2,** 171–178.

Henning, K.H. and Störr, H. (1986) *Electron Micrographs (TEM, SEM) of Clays and Clay Minerals.* Akademia-Verlag Press, Berlin, 350 pp.

Hover, V.C., Walter, L.M., Peacor, D.R., and Martini, A.M. (1999) Mg-smectite authigenesis in a marine evaporative environment, Salina Ornetepec, Baja California. *Clays and Clay Minerals,* **47,** 252–268.

Kistler, R.B. and Helvacı, C. (1994) Boron and borates. In *Industrial Minerals and Rocks, 6th edition,* D.D. Carr, ed., Society of Mining, Metallurgy and Exploration, Inc, Littleton, Colorado, 171–178.

Lange, B. and Vejdelek, Z.J. (1980) *Photometrische Analyse.* Verlag Chemie, Altenberg, 455 pp.

Maxwell, D.T. and Hower, J. (1967) High-grade diagenesis and low-grade metamorphism of illite in the Precambrian Belt Series. *American Mineralogist,* **52,** 843–857.

Özpeker, I. (1969) Bati Anadolu borat yataklarının mukayeseli jenetik etüdü. Ph.D. thesis, İstanbul Technical University, İstanbul, 116 pp.

Semelin, B., and Yalçın, H. (1984) Sedimentation volcanoclastique en milieu continental lacustre: Un exemple, le bassin Neogene d'Emet (Turquie Ouest). *Abstract, 5eme Congress European de Sedimentologie, Marseille, 9–11 April,* 403.

Velde, B. (1992) *Introduction to Clay Minerals: Chemistry, Origins, Uses and Environmental Significance.* Chapman and Hall, London, 198 pp.

Weaver, C.E. and Pollard, L.D. (1975) *The Chemistry of Clay Minerals. Developments in Sedimentology, Volume, 15,* Elsevier, Amsterdam, 213 pp.

Yalçin, H. (1984) Emet Neojen gölsel baseninin jeolojik ve mineralojik petrografik incelenmesi. M.S. thesis, Hacettepe University, Ankara, 269 pp.

Yalçın, H. and Gündoğdu, M.N. (1985) *Emet gölsel Neojen baseninin kil mineralojisi. II. Ulusal Kil Sempozyumu Bildirileri,* M.N. Gündogdu and H. Aksoy, eds., Hacettepe University, Ankara, 155–170.

E-mail of corresponding author: Mumtaz35@hotmail.com

(Received 16 July 1998; accepted 23 February 2000; Ms. 98-100; A.E. W. Crawford Elliott; A.E. Warren D. Huff)